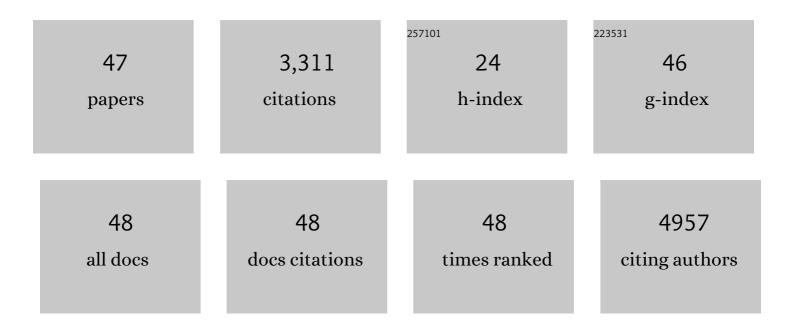
Eric Schaible

List of Publications by Year in descending order

Source: https://exaly.com/author-pdf/653988/publications.pdf Version: 2024-02-01



#	Article	IF	CITATIONS
1	A SAXS/WAXS/GISAXS Beamline with Multilayer Monochromator. Journal of Physics: Conference Series, 2010, 247, 012007.	0.3	522
2	Age-related changes in the plasticity and toughness of human cortical bone at multiple length scales. Proceedings of the National Academy of Sciences of the United States of America, 2011, 108, 14416-14421.	3.3	325
3	On the tear resistance of skin. Nature Communications, 2015, 6, 6649.	5.8	297
4	Mechanical adaptability of the Bouligand-type structure in natural dermal armour. Nature Communications, 2013, 4, 2634.	5.8	277
5	Characterization of the effects of x-ray irradiation on the hierarchical structure and mechanical properties of human cortical bone. Biomaterials, 2011, 32, 8892-8904.	5.7	250
6	In situ dynamic observations of perovskite crystallisation and microstructure evolution intermediated from [PbI6]4â^ cage nanoparticles. Nature Communications, 2017, 8, 15688.	5.8	191
7	Protective role of Arapaima gigas fish scales: Structure and mechanical behavior. Acta Biomaterialia, 2014, 10, 3599-3614.	4.1	161
8	Fracture resistance of human cortical bone across multiple length-scales at physiological strain rates. Biomaterials, 2014, 35, 5472-5481.	5.7	125
9	Fast Printing and In Situ Morphology Observation of Organic Photovoltaics Using Slotâ€Đie Coating. Advanced Materials, 2015, 27, 886-891.	11.1	117
10	In Situ Morphology Studies of the Mechanism for Solution Additive Effects on the Formation of Bulk Heterojunction Films. Advanced Energy Materials, 2015, 5, 1400975.	10.2	102
11	Characterizing the nano and micro structure of concrete to improve its durability. Cement and Concrete Composites, 2009, 31, 577-584.	4.6	91
12	Intrinsic mechanical behavior of femoral cortical bone in young, osteoporotic and bisphosphonate-treated individuals in low- and high energy fracture conditions. Scientific Reports, 2016, 6, 21072.	1.6	65
13	Novel Defense Mechanisms in the Armor of the Scales of the "Living Fossil―Coelacanth Fish. Advanced Functional Materials, 2018, 28, 1804237.	7.8	61
14	Alendronate treatment alters bone tissues at multiple structural levels in healthy canine cortical bone. Bone, 2015, 81, 352-363.	1.4	58
15	Contributions of Material Properties and Structure to Increased Bone Fragility for a Given Bone Mass in the UCD-T2DM Rat Model of Type 2 Diabetes. Journal of Bone and Mineral Research, 2018, 33, 1066-1075.	3.1	57
16	Morphology and Optical Properties of P3HT:MEH-CN-PPV Blend Films. Macromolecules, 2013, 46, 4491-4501.	2.2	47
17	Structure and Mechanical Adaptability of a Modern Elasmoid Fish Scale from the Common Carp. Matter, 2020, 3, 842-863.	5.0	47
18	Real-time X-ray scattering studies of film evolution in high performing small-molecule–fullerene organic solar cells. Journal of Materials Chemistry A, 2015, 3, 8764-8771.	5.2	42

ERIC SCHAIBLE

#	Article	IF	CITATIONS
19	Mechanical Competence and Bone Quality Develop During Skeletal Growth. Journal of Bone and Mineral Research, 2019, 34, 1461-1472.	3.1	41
20	Topological Effects on Globular Proteinâ€ELP Fusion Block Copolymer Selfâ€Assembly. Advanced Functional Materials, 2015, 25, 729-738.	7.8	40
21	An <i>in situ</i> GISAXS study of selective solvent vapor annealing in thin block copolymer films: Symmetry breaking of inâ€plane sphere order upon deswelling. Journal of Polymer Science, Part B: Polymer Physics, 2016, 54, 331-338.	2.4	40
22	Chronic kidney disease and aging differentially diminish bone material and microarchitecture in C57Bl/6 mice. Bone, 2019, 127, 91-103.	1.4	37
23	Evolution of Ordered Metal Chalcogenide Architectures through Chemical Transformations. Journal of the American Chemical Society, 2013, 135, 7446-7449.	6.6	30
24	Noninvasive histological comparison of bone growth patterns among fossil and extant neonatal elephantids using synchrotron radiation X-ray microtomography. Journal of Vertebrate Paleontology, 2012, 32, 939-955.	0.4	27
25	Correlations between Salt-Induced Crystallization, Morphology, Segmental Dynamics, and Conductivity in Amorphous Block Copolymer Electrolytes. Macromolecules, 2018, 51, 1733-1740.	2.2	27
26	Effect of sequential treatments with alendronate, parathyroid hormone (1–34) and raloxifene on cortical bone mass and strength in ovariectomized rats. Bone, 2014, 67, 257-268.	1.4	24
27	In Situ X-ray Scattering Studies of the Influence of an Additive on the Formation of a Low-Bandgap Bulk Heterojunction. Chemistry of Materials, 2017, 29, 2283-2293.	3.2	23
28	Ordering in Polymer Micelle-Directed Assemblies of Colloidal Nanocrystals. Nano Letters, 2015, 15, 8240-8244.	4.5	21
29	Thermal stability and thermal aging of poly(vinyl chloride)/MgAl layered double hydroxides composites. Chinese Journal of Polymer Science (English Edition), 2016, 34, 542-551.	2.0	21
30	High-yield growth kinetics and spatial mapping of single-walled carbon nanotube forests at wafer scale. Carbon, 2020, 159, 236-246.	5.4	15
31	Mechanically tunable elastomer and cellulose nanocrystal composites as scaffolds for <i>in vitro</i> cell studies. Materials Advances, 2021, 2, 464-476.	2.6	15
32	On the Origins of Fracture Toughness in Advanced Teleosts: How the Swordfish Sword's Bone Structure and Composition Allow for Slashing under Water to Kill or Stun Prey. Advanced Science, 2019, 6, 1900287.	5.6	14
33	Dynamic Structure and Phase Behavior of a Block Copolymer Electrolyte under dc Polarization. ACS Applied Materials & Interfaces, 2020, 12, 57421-57430.	4.0	13
34	Note: Setup for chemical atmospheric control during <i>in situ</i> grazing incidence X-ray scattering of printed thin films. Review of Scientific Instruments, 2017, 88, 066101.	0.6	13
35	Liquid-free covalent reinforcement of carbon nanotube dry-spun yarns and free-standing sheets. Carbon, 2022, 187, 415-424.	5.4	11
36	Nanocrystal Superlattice Embedded within an Inorganic Semiconducting Matrix by in Situ Ligand Exchange: Fabrication and Morphology. Chemistry of Materials, 2015, 27, 2755-2758.	3.2	10

ERIC SCHAIBLE

#	Article	IF	CITATIONS
37	Effect of block copolymer morphology on crystallization and water transport. Polymer, 2017, 120, 209-216.	1.8	10
38	Effect of crystallization of the polyhedral oligomeric silsesquioxane block on self-assembly in hybrid organic-inorganic block copolymers with salt. Giant, 2021, 6, 100055.	2.5	10
39	Soot-particle core-shell and fractal structures from small-angle X-ray scattering measurements in a flame. Carbon, 2022, 196, 440-456.	5.4	10
40	The role of collagen in the dermal armor of the boxfish. Journal of Materials Research and Technology, 2020, 9, 13825-13841.	2.6	7
41	Electrophoresis Assisted Printing: A Method To Control the Morphology in Organic Thin Films. ACS Applied Materials & Interfaces, 2020, 12, 5219-5225.	4.0	6
42	Distinguishing Gas-Phase and Nanoparticle Contributions to Small-Angle X-ray Scattering in Reacting Aerosol Flows. Journal of Physical Chemistry A, 2022, 126, 3015-3026.	1.1	6
43	Nanolatticed Architecture Mitigates Damage in Shark Egg Cases. Nano Letters, 2021, 21, 8080-8085.	4.5	2
44	Printing Fabrication of Bulk Heterojunction Solar Cells and In Situ Morphology Characterization. Journal of Visualized Experiments, 2017, , .	0.2	1
45	Modulation of Carrier Type in Nanocrystal-in-Matrix Composites by Interfacial Doping. Chemistry of Materials, 2018, 30, 2544-2549.	3.2	1
46	Biomimetics: On the Origins of Fracture Toughness in Advanced Teleosts: How the Swordfish Sword's Bone Structure and Composition Allow for Slashing under Water to Kill or Stun Prey (Adv. Sci.) Tj ETQq0 0 0 rgB	[/@.werlock	2 110 Tf 50 37

47Nanolattice-Forming Hybrid Collagens in Protective Shark Egg Cases. Biomacromolecules, 2022, 23,
2878-2890.2.60